

reducing agent other than CO, e.g. Zn, which can also serve as a chloride acceptor.

If structure **2a** is correct for the adsorbed tricarbonyl on SiO₂ and NaY, then there should be no reaction between the adsorbed carbonyl chloride and CO at room temperature, since there is nothing that can serve as a chloride acceptor. This is indeed the case; no reaction is observed between **2a** and CO (25 °C, 1 atm) after 24 h.

Similarly, a reaction is to be expected between **2b** on MgO and CO at room temperature. Although a reaction does occur, it is unfortunately not nearly as clean as previously observed on Al₂O₃. Thus, when **2b** on MgO is treated with CO, a very complicated infrared spectrum is obtained. Some of the bands may be due to [HRu₃(CO)₁₁]⁻(ads), but if this anion is present, it is not the major product. That a reaction takes place at all however is consistent with MgO acting as a chloride acceptor.

Conclusion

Although Ru(CO)₃Cl₂(THF) is spontaneously adsorbed by a

number of oxides, it is impossible to determine the surface structure of the adsorbed species simply by the infrared spectrum. Thus, a previous study on silica assigned the surface structure as Ru^{II}(CO)₃(ads), a structure that does not contain coordinated chloride. It is apparent from the present study that a better description of the surface carbonyl on SiO₂ and NaY zeolite is Ru(CO)₃Cl₂(ads). Only on the more basic oxides, Al₂O₃ and MgO, is chloride lost to yield the surface species Ru^{II}(CO)₃(ads). It is further proposed that the surface ligands include two oxides, O-Al, so that the adsorbed tricarbonyl is not a formally cationic complex. Importantly, the distinction between the two surface structures is not readily made simply from the infrared spectra. The basic chemical reactions of the adsorbed carbonyls are required to confirm the proposed structures.

Acknowledgment. Support for this work was provided by the National Science Foundation (Grant DMR 85-18364). B.E.H. acknowledges an A. von Humboldt fellowship during part of this work.

Contribution from the Department of Chemistry,
Cornell University, Ithaca, New York 14853

Synthesis, Structure, and Properties of a New Ternary Metal Nitride, Ca₃CrN₃

Deborah A. Vennos, Michael E. Badding, and F. J. DiSalvo*

Received February 27, 1990

We have synthesized a new ternary nitride, Ca₃CrN₃, from the binary nitrides at high temperature. The refined structure was solved in the *Cmcm* space group, *Z* = 4, with lattice constants (Å) *a* = 8.503 (2), *b* = 10.284 (2), and *c* = 5.032 (1) and with *R* = 3.9% and *R_w* = 3.9%. This new structure type consists of sheets of [CrN₃]⁶⁻ planar triangular units and calcium ions. Ca₃CrN₃ is insulating and paramagnetic with Cr³⁺ in the low-spin state. This is the first unambiguous example of low-spin Cr³⁺. Larger than expected antiferromagnetic interactions produce a maximum in the magnetic susceptibility at 240 K, even though the shortest Cr-Cr distance is 4.73 Å.

Introduction

Although the chemistry of binary nitrides has been explored in detail, comparatively little work on ternary and quaternary nitrides has been reported. Preliminary work has shown that, in addition to the facile formation and stability of ternary nitrides containing electropositive elements, these phases exhibit a variety of novel properties. Examples include the Ni d⁹ configuration in CaNiN,¹ the layered structures of MTaN₂² (*M* = alkali metal), and the unique structure types found in Ca₂₁Fe₃N₁₇,³ Li₃AlN₂,⁴ and CaGaN.⁵ These few examples suggest that ternary nitrides will display an extensive assortment of new compounds and structure types. We therefore undertook a large-scale investigation of alkaline-earth-metal- and transition-metal-containing nitrides.

Herein, we report a new compound and structure type, Ca₃CrN₃, discovered initially as an impurity phase in reactions of Ca₃N₂ in stainless steel containers.

Experimental Section

Starting Materials. Chromium nitride was prepared by heating Cr powder (-100 mesh, 3N) in flowing nitrogen (prepurified by passing through finely divided copper at 150 °C and then activated alumina) at 800 °C for 1 day. The product was ground and reheated several times, yielding a mixture of CrN and Cr₂N (approximately 50:50). Granules of calcium (2N) were reacted at 1000 °C for 3 days in flowing nitrogen

(prepurified as above) to yield pure Ca₃N₂. The binary products were identified by X-ray powder diffraction methods. Since both Ca₃N₂ and Ca₃CrN₃ are air sensitive, all manipulations were carried out in an argon-filled glovebox.

Synthesis of Ca₃CrN₃. The title compound was first discovered as a minority crystalline phase in a reaction of Ca₃N₂ and tin in a stainless steel tube. The bulk phase consisted of a gray powder, Ca₃SnN₆,⁶ with a minority phase consisting of needle crystals distributed throughout. Microprobe analysis of the crystals indicated the presence of calcium and chromium (a component in the stainless steel) at a Ca:Cr molar ratio of 3:1.

The compound was then prepared as a majority phase by heating 0.2048 g of the CrN/Cr₂N mixture (1.11 mmol of the hypothetical Cr₃N₂) and 0.6011 g of Ca₃N₂ (4.06 mmol) in a sealed stainless steel tube under an argon atmosphere at 1350 °C for 4 days, followed by cooling to 1050 °C in 5 h and finally cooling to room temperature in 12 h. There was no evidence of Ca₃N₂ remaining in the product mixture; however, the brittle nature of the once malleable tube indicated that the excess Ca₃N₂ was consumed by a reaction with the stainless steel. The product contained air-sensitive, burgundy needle crystals up to 1 mm in length, which were used for the structure determination. X-ray powder diffraction indicated a nearly pure Ca₃CrN₃ powder with a small unidentified impurity phase. The intensity of the strongest impurity diffraction peak was 6% as intense as the strongest peak of the majority phase.

The material used for susceptibility measurements was prepared by heating a pressed pellet of an intimate mixture of 0.3103 g of CrN/Cr₂N (1.69 mmol of Cr₃N₂) and 0.5070 g of Ca₃N₂ (3.43 mmol) powders in a sealed molybdenum crucible under argon at the heating schedule mentioned above. The only impurity observable in the product by powder X-ray diffraction was Cr metal. The most intense Cr peak was only 6%

(1) Chern, M. Y.; DiSalvo, F. J. Submitted for publication in *J. Solid State Chem.*

(2) Jacobs, H.; von Pinkowski, E. *J. Less-Common Met.* **1989**, *146*, 147.

(3) Verdier, P.; Marchand, R.; Lang, J. *Rev. Chim. Miner.* **1976**, *13*, 214.

(4) Juza, V. R.; Hund, F. Z. *Anorg. Allg. Chem.* **1948**, *257*, 13.

(5) Verdier, P.; L'Haridon, P.; Maunay, M.; Marchand, R. *Acta Crystallogr.* **1974**, *30*, 226.

(6) Chern, M. Y.; Vennos, D. A.; DiSalvo, F. J. To be published.

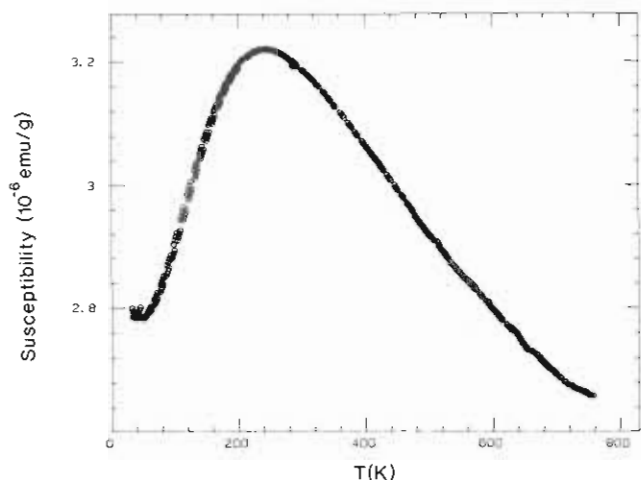


Figure 1. Temperature dependence of the magnetic susceptibility of Ca_3CrN_3 .

Table I. Summary of Crystal and Diffraction Data for Ca_3CrN_3

space group	$Cmcm$ (No. 63)
Z	4
$a, b, c, \text{\AA}$	8.503 (2), 10.284 (2), 5.032 (1)
$V, \text{\AA}^3$	440
cryst dimens, mm	$0.03 \times 0.04 \times 0.13$
2θ max, deg; scan type	55; $\omega-2\theta$
octants measd	$\pm h, k, l$
X-ray radiation	$\text{Mo K}\alpha$
monochromator	graphite
no. of measd reflns	577
no. of obsd reflns ^a	303
no. of independent reflns	263
abs coeff μ, mm^{-1}	5.79
$R, {}^b R_w, {}^c \%$	3.9, 3.9

^a $F_o^2 > 3s(F_o^2)$. ^b $R = \sum(|F_o| - |F_c|) / \sum(|F_o|)$. ^c $R_w = [\sum(w|F_o| - |F_c|)^2] / \sum(w|F_o|^2)]^{1/2}$; $w = s(F_o)^{-2}$.

as intense as the strongest Ca_3CrN_3 peak. Since the lower symmetry of Ca_3CrN_3 splits the X-ray lines into many components, the impurity level of Cr was estimated to be less than 3 wt %. A larger percentage of Cr from the reaction mixture should have remained in the product; most of it must have alloyed with the molybdenum crucible, as it is not observed in the product.

Magnetic Susceptibility. The magnetic susceptibility of the sample was measured by the Faraday technique in a previously calibrated system.⁷ The susceptibility of a sample sealed in a thin-walled quartz tube was determined to be field independent at room temperature, showing that no ferromagnetic impurities were present. Figure 1 shows the results of a temperature-dependent study between 30 and 750 K at a magnetic field strength of 14.2 kG.

The contribution of the <3 wt % Cr impurity to the observed peak in the susceptibility is negligible, since its gram susceptibility is approximately 3×10^{-6} emu/g and weakly temperature dependent, increasing by only 10% from 0 to 800 K.⁸

Electrical Properties. The resistance of a pellet of Ca_3CrN_3 was measured in a small press inside the glovebox. The two pistons were electrically insulated from each other, allowing a two-point measurement of the resistance. The resistance determined on a pellet 4.5 mm in diameter and approximately 3 mm thick was 45 k Ω .

Structure Determination. Unit cell symmetry and approximate lattice constants were obtained from Weissenberg photographs of a crystal mounted along the needle axis. A $0.03 \times 0.04 \times 0.13$ mm³ crystal, sealed in a glass capillary under argon, was used in the structure determination. Data were collected on a Syntex P2₁ diffractometer using $\text{Mo K}\alpha$ radiation and a graphite monochromator. The choice of space groups was reduced to $Cmcm$, $Cmc2_1$, and $C2cm$ by systematic absences, and the structure was solved by using direct methods in the $Cmcm$ space group. Refinement in either noncentrosymmetric space group resulted in no

Table II. Positional Parameters for Ca_3CrN_3

atom	site	x	y	z
Ca	4c	0	0.1079 (2)	0.25
Ca	8g	0.2843 (2)	-0.1174 (1)	0.25
Cr	4c	0.5	0.1945 (2)	0.25
N	4c	0.5	0.3757 (8)	0.25
N	8g	0.6918 (8)	0.1286 (6)	0.25

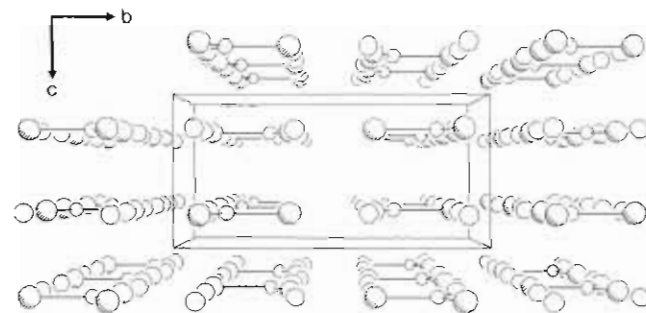


Figure 2. View of the structure down the a axis. The Ca atoms are open circles, Cr atoms are dotted circles, and N atoms are partially hatched circles.

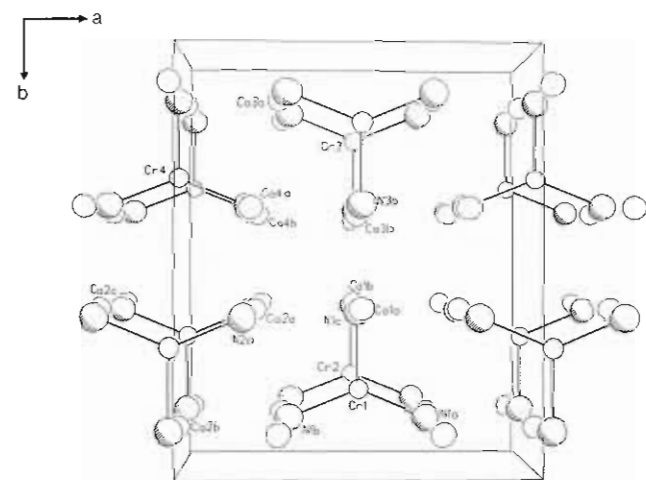


Figure 3. View of Ca_3CrN_3 down the c axis, showing one unit cell and indicating the labels used to identify the atoms in Table III.

significant change in the structure or R factors. An empirical absorption correction (the ψ -scan method) was performed, and two octants of data were collected and merged to improve the data set. The largest peak in the final difference Fourier map was 0.86 e. Final $R = 3.9\%$ and $R_w = 3.9\%$ were obtained after refinement. The structure determination and refinement were performed by using Nicolet SHELXTL Plus software running on a Microvax computer. Table I summarizes data collection parameters. Atomic positions are listed in Table II.

After the structure was solved, the powder patterns taken on a Scintag XDS2000 diffractometer could be indexed. The observed patterns matched that calculated by Lazy Pulverix,⁹ on the basis of the single-crystal data.

Results and Discussion

The structure of Ca_3CrN_3 (Figures 2 and 3) consists of triangular $[\text{CrN}_3]^{6-}$ units with C_{2v} point symmetry separated by calcium atoms (the C_{2v} axis is parallel to the b axis). A view down the a axis clearly shows the sheet structure of the planar groups and the intervening Ca atoms. In each sheet the triangular units are pointing in the same direction. Neighboring sheets are displaced by $1/2$ in z , and the orientation of the triangles is reversed.

A list of relevant bond distances and angles can be found in Table III.

Although the triangular planar coordination of a transition metal by nitrogen has been observed in molecular solids,^{10,11} this

(7) Vassiliou, J.; Hornbostel, M.; Ziebarth, R.; DiSalvo, F. J. *J. Solid State Chem.* **1989**, *81*, 208.

(8) Vogt, E.; Hohl, M. *Zahlenwerte und Funktionen aus Physik Chemie Astronomie Geophysik Technik*, 6th ed.; Landolt, Bornstein, Eds.; Springer-Verlag: Berlin, 1962; Vol. 2, pp 1-8.

(9) Yvon, K.; Jeitschko, W.; Parthe, E. *J. Appl. Crystallogr.* **1977**, *10*, 73.

(10) Bradley, D. C.; Chisholm, M. H. *Acc. Chem. Res.* **1976**, *9*, 273.

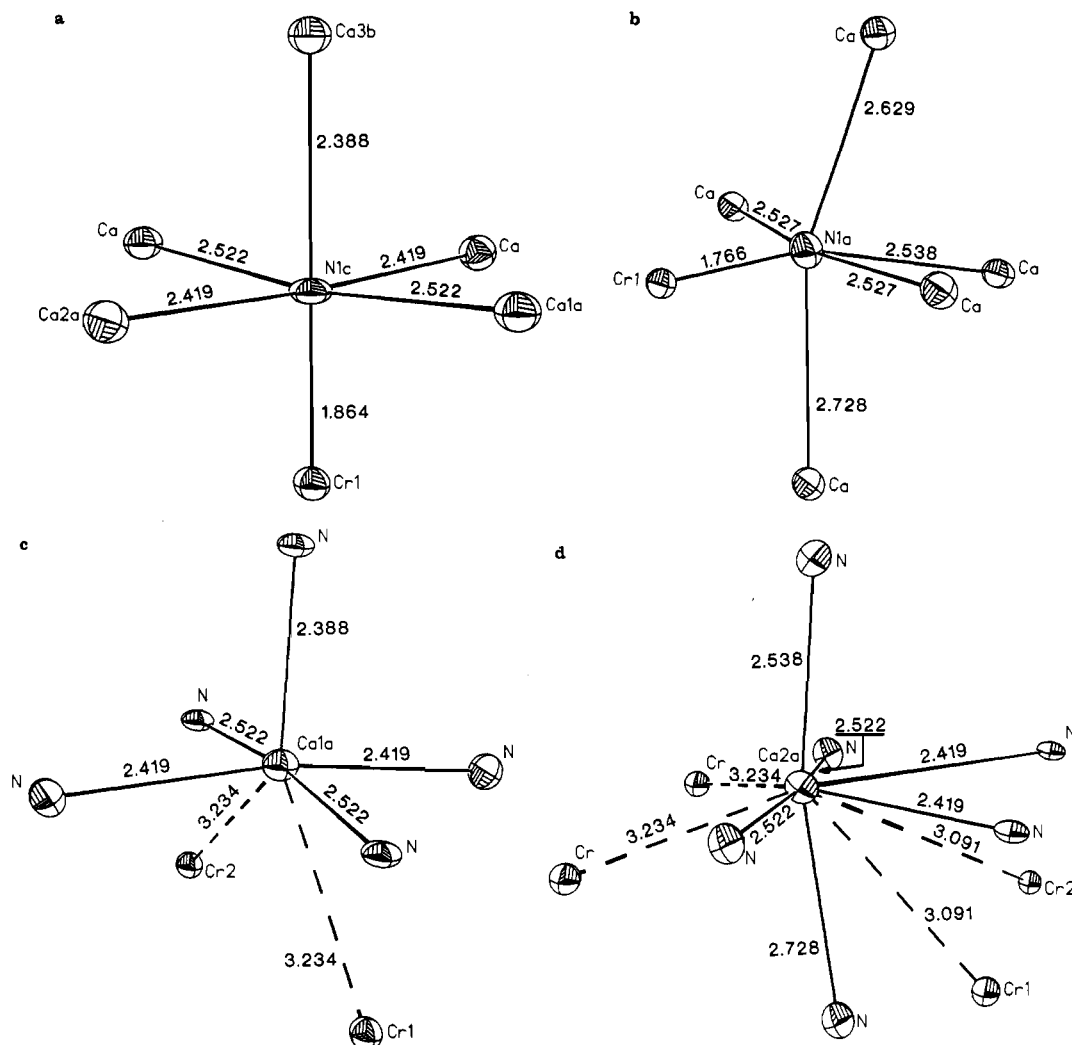


Figure 4. (a) Distorted octahedral environment of the unique nitrogen atom (N(1c)). (b) Coordination about the equivalent nitrogen atoms (N(1a), N(1b)). (c) Local environment about the unique calcium atom (Ca(1a)). (d) Irregular coordination about the equivalent calcium atoms (Ca(2a), Ca(2c)).

Table III. Important Distances (Å) and Angles (deg) in Ca₃CrN₃

Nonbonding Interactions			
Cr(1)···Cr(2)	5.032 (1)	Ca(1b)···Ca(4b)	3.349 (2)
Cr(1)···Cr(3)	4.726 (1) ^a	Ca(2b)···Ca(2c)	3.368 (3)
Cr(1)···Ca(1a)	3.234 (2)	Ca(2b)···Ca(3a)	3.491 (1) ^a
Cr(1)···Ca(1b)	3.234 (2)	Ca(2a)···Ca(2c)	3.668 (4)
Cr(1)···Ca(3a)	3.213 (1) ^a	Ca(2a)···Ca(3a)	3.757 (2)
Cr(4)···Ca(2a)	3.695 (2)	Ca(2a)···Ca(4b)	3.487 (2)
Ca(1b)···Ca(3b)	3.355 (3)		
Bonding Interactions			
Cr(1)–N(1b)	1.766 (7)	Ca(2a)–N(1c)	2.419 (2)
Cr(1)–N(1a)	1.766 (7)	Ca(2a)–N(1b)	2.728 (6)
Cr(1)–N(1c)	1.864 (8)	Ca(2b)–N(1b)	2.629 (7)
Ca(1a)–N(1c)	2.522 (1)	Ca(3b)–N(1c)	2.388 (8)
Ca(1b)–N(1c)	2.522 (1)	Ca(4a)–N(2a)	2.538 (6)
Bond Angles			
N(1a)–Cr(1)–N(1c)	112.6 (2)	N(1b)–Cr(1)–N(1a)	134.9 (4)
N(1b)–Cr(1)–N(1c)	112.6 (2)		

^aDistance indicated is from an atom in the unit cell shown to an atom in an adjacent unit cell, respectively.

is the first example of such coordination in the solid state. The coordination geometry around the nitrogens is a distorted octahedron, consisting of four "equatorial" Ca's, one "axial" Ca, and one "axial" Cr. The bond lengths about the unique N (N(1c) in Figures 3 and 4a) are 2×2.522 Å, 2×2.419 Å, and 2.388 Å

to Ca and 1.864 Å to Cr. The two equivalent nitrogens (N(1a) and N(1b) in Figures 3 and 4b) have similar bond lengths, but the octahedral angles are considerably distorted from 90° , and the Cr–N bond lengths are compressed to 1.766 Å. The environment about the unique calcium (Ca(1a) in Figures 3 and 4c) can be approximated as a square pyramid of nitrogens with two additional long Ca–Cr bonds. However, the environment about the two equivalent calciums (Ca(2a) and Ca(2c) in Figures 3 and 4d) is quite irregular with 6-fold coordination to nitrogen.

There are very few compounds with Cr–N bonds with which to compare distances. The Cr–N bond lengths in molecular solids range from a Cr–N formal triple bond (1.57 Å)¹² to apparent single bonds in the range 2.04 – 2.25 Å.^{13–19} In the solid state, Cr–N bond lengths average considerably larger (2.06 – 2.93 Å).^{20–22} The Cr–N distances in the [CrN₃]⁶⁻ unit indicate multiple metal

(11) Bradley, D. C.; Hursthouse, M. B.; Newing, C. W. *Chem. Commun.* **1971**, 8, 411.

(12) Groves, J. T.; Takahashi, T.; Butler, W. M. *Inorg. Chem.* **1983**, *22*, 884.
 (13) Bush, M. A.; Sim, G. A. *J. Chem. Soc. A* **1970**, *4*, 605.
 (14) Greenhough, T. J.; Kolthammer, B. W.; Legzdins, P.; Trotter, J. *Inorg. Chem.* **1979**, *18*, 3548.
 (15) Bino, A.; Cotton, F. A.; Kaim, W. *Inorg. Chem.* **1979**, *18*, 3566.
 (16) Richeson, D. S.; Mitchell, J. F.; Theopold, K. H. *Organometallics* **1989**, *8*, 2570.
 (17) Ball, R. G.; Hames, B. W.; Legzdins, P.; Trotter, J. *Inorg. Chem.* **1980**, *19*, 3626.
 (18) Albrecht, V. G. *Z. Chem.* **1963**, *3*, 182.
 (19) Ford, P. D.; Larkworthy, L. F.; Povey, D. C.; Roberts, A. J. *Bull. Soc. Chim. Fr.* **1983**, *2*, 1983.
 (20) Aivazov, M. I.; Rezhikova, T. V. *Russ. J. Inorg. Chem. (Engl. Transl.)* **1977**, *22*, 250.
 (21) Eddine, M. N.; Bertaut, E. F.; Roubin, M.; Paris, J. *Acta Crystallogr., Sect. B* **1977**, *33B*, 3010.
 (22) Juzar, R. V.; Jurgen, H. *Z. Anorg. Allg. Chem.* **1961**, *309*, 276.

to nitrogen bonding in comparison to the average Cr–N single bond distances in molecular solids. The closest Ca–Ca distance between the planar units (3.36 Å) is slightly longer than that in Ca_3N_2 (3.16 Å).²³ However, the closest Ca–N distances (2.38, 2.54 Å) are similar to those in Ca_3N_2 (2.46 Å),²³ Ca_3BiN (2.45 Å),⁶ and CaNiN (2.50 Å).¹

The Cr–Cr distances are much too long for any metal–metal bonding or significant direct exchange interactions. The shortest distance, 4.73 Å, is between Cr in adjacent sheets (Cr(1) or Cr(2) to Cr(3) in the unit cell below the one shown in Figure 3). The next closest distances are 5.03 Å (Cr(1) to Cr(2), across two sheets) and 5.06 Å (Cr(3) to Cr(4) in Figure 3).

These long Cr–Cr distances suggest a very small exchange interaction between paramagnetic Cr^{3+} ions. Consequently, we expected the susceptibility to follow a simple Curie–Weiss law, where the susceptibility is equal to $C/(T + \theta)$ and θ is expected to be less than 10 K. We ignore the small temperature-independent term expected in the susceptibility, since it is a sum of a small diamagnetic term (the core diamagnetism, between -0.2×10^{-6} and -0.33×10^{-6} emu/g,²⁴ depending upon the poorly established value of the core diamagnetism for N in solids) and a small paramagnetic term (the van Vleck paramagnetism, which is unknown). The fact that the susceptibility does not follow the simple Curie–Weiss law (at least below approximately 400 K) suggests that strong antiferromagnetic superexchange interactions must follow paths such as Cr–N···N–Cr or Cr–N–Ca–N–Cr. The lack of a sharp break in the susceptibility implies that three-dimensional long-range order of the Cr spins does not occur above 30 K. The broad peak in the susceptibility therefore suggests moderately strong antiferromagnetic interactions in only one or two dimensions.²⁵ Since the optimal exchange pathways are not obvious, it is not possible to be certain about the dimensionality of the exchange interactions. However, if the dominant exchange is between closest neighbor Cr atoms, then the exchange pathway forms a zigzag chain parallel to the *c* axis. The next closest Cr–Cr distances are only 0.3 Å longer; consequently, our assignment of the optimal exchange path may not be correct.

In principle, the magnetic susceptibility can be used to determine the spin of the Cr. Since the Cr site symmetry is so low, none of the Cr *d* states are degenerate. Depending upon their relative splittings, the Cr^{3+} could be high spin ($S = 3/2$) or low spin ($S = 1/2$). If the exchange is Heisenberg-like and one-dimensional, the product of the molar susceptibility at the maximum and the

temperature of the maximum is a function only of the spin.²⁵ The maximum molar susceptibility is 6.85×10^{-4} emu/mol, and the temperature at the maximum is 240 K. The product, 0.164 emu·K/mol, is close to that expected for $S = 1/2$ (0.141 emu·K/mol) but much smaller than that expected for $S = 3/2$ (0.648 emu·K/mol).²⁵ Since the experimental value is not exactly equal to the theoretical number for $S = 1/2$, other exchange pathways may also be important.

At very high temperatures the effective moment per Cr theoretically must extrapolate to the free ion value. At the highest temperature of measurement we obtain $1.86 \mu_B$, somewhat above the expected infinite temperature $\text{spin-}1/2$ value of $1.73 \mu_B$ but considerably below the $\text{spin-}3/2$ value of $3.87 \mu_B$. The source of the small discrepancy is not clear but could be caused by a van Vleck susceptibility that is larger than the core diamagnetism or by a small thermal population of the excited $\text{spin-}3/2$ state. In any case, the spin state of Cr^{3+} in this compound is clearly low-spin $S = 1/2$.

The exchange energy, *J*, is also obtainable from the temperature of the maximum.²⁵ We obtain $J = 185 \pm 5$ K. It is surprising to us that such a large exchange can occur between paramagnetic centers almost 5 Å apart. This is likely due to a large covalent contribution to the bonding and overlaps from one Cr to the next, although we did not expect the exchange to be so large, as previously discussed.

To our knowledge this is the first unambiguous example of a low-spin Cr^{3+} compound. One previous publication²⁶ on chromium-doped silicates suggests that chromium occupies both octahedral and tetrahedral sites and that the tetrahedrally coordinated Cr^{3+} is low spin, but we could find no references to a concentrated chromium compound that contained such low-spin species.

To summarize, the new phase Ca_3CrN_3 has been prepared by reaction of the binary nitrides at high temperature. The compound represents a new structure type, consisting of triangular planar $[\text{CrN}_3]^{6-}$ units separated by calcium atoms. It is a paramagnetic insulator with low-spin Cr^{3+} and low-dimensional antiferromagnetic interactions.

Acknowledgment. We wish to extend appreciation to Greg VanDuyne of the Cornell Chemistry X-ray Facility for assistance with the structure determination. D.A.V. would like to express gratitude to Ming Y. Chern for his generous help in getting started with the nitrides. Support of this work through the Office of Naval Research is greatly appreciated.

Supplementary Material Available: For Ca_3CrN_3 , a table of refined anisotropic thermal parameters (1 page); a table of observed and calculated structure factors (1 page). Ordering information is given on any current masthead page.

(23) Laurent, Y.; Lang, J.; LeBihan, M. T. *Acta Crystallogr., Sect. B* **1968**, *24B*, 494.

(24) Selwood, P. W. *Magnetochemistry*; Wiley Interscience: New York, 1979.

(25) Hatfield, W. E. In *Solid State Chemistry: Techniques*; Cheetham, A. K., Day, P., Eds.; Oxford Science Publications: London, 1987; Chapter 4.

(26) Ikeda, K. *Kobutsugaku Zasshi* **1984**, *16* (5), 385.